https://doi.org/10.32056/KOMAG2022.4.7

Influence of nonlinearities in sensor and actuator on the operation of the rotational speed control system of a roadheader cutting head

Received: 27.12.2022

Accepted: 29.12.2022

Published online: 30.12.2022

Author's affiliations and addresses:

[1] Silesian University of Technology, Faculty of Mining, Safety Engineering and Industrial Automation, Akademicka 2a, 44-100 Gliwice, Poland

*** Correspondence:**

e-mail: jaroslaw.joostberens@polsl.pl

Jarosław JOOSTBERENS [1*], Adam HEYDUK [1]

Abstract:

The paper presents a discussion on the selected nonlinearities existing in sensor and actuator subsystems of the roadheader cutting head speed control system. There have been concerned the most significant nonlinearities - rotational speed encoder and frequency rate limiter in the input of the power electronic converter. There has been presented a detailed analysis of the nonlinear input frequency rate limiter and the frequency-dependent input-output curves have been calculated. They enable qualitative and quantitative evaluation of system performance over a wide range of input signal frequencies and amplitudes. The measurement time of the encoder-based speed sensing should be as short as possible, or continuous measurement (like tachogenerator) should be used. The impact of encoder delay and inertia is much less significant than that of the frequency rate limiter. For better drive system performance, the frequency converter should be overmatched to ensure current overload capability – allowing an increase in the permissible rate of output voltage frequency change.

Keywords: roadheader, speed control system, rotational encoder, power electronic converter, rate limiter, describing function.

1. Introduction

Roadheaders are large-power complex machines commonly used in underground mining and tunnelling [1]. Modern mining machines (including longwall shearers and roadheaders) are sophisticated mechatronic systems [2], in which the operation of the electronic control system has a significant impact on their performance and achieved production results. Thus, it is advisable to search for methods of optimizing their operation taking into account both mathematical models [3] and the results of their empirical tests [4]. The main research and development directions include arm position control [5], cutting head geometry optimization [6], sensor fusion [7], load condition identification [8,9] and the application of machine vision systems [10,11]. Methods based on artificial intelligence (neural networks) are often used [12,13]. The problem described in this paper emerged during the implementation of a research project of an innovative R-130 roadheader (manufactured by FAMUR S.A.) with an inverter-fed drive of the cutting head. As the rock cutting process is a complex combination of many stochastic (resulting from the fracture of brittle, stratified material) and deterministic factors (specified by the arrangement of the picks on the cutting head surface), the evaluation of this process, in order to determine the optimum value of rotational speed minimizing the power consumption of the process and limiting the frequency of significant dynamic overloads, can only be performed over longer periods of time (corresponding, for example, to one cutting head rotation time). This process is illustrated in Fig. 1.

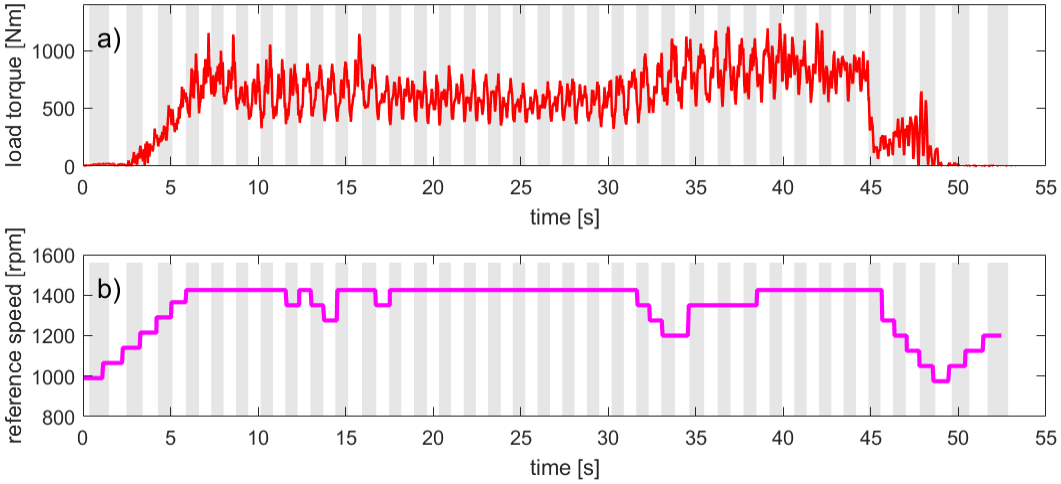

Fig. 1. An example of reference speed generator operation recorded at the laboratory stand: a) recorded load torque, b) generated reference speed

The task of the speed control system is then to track these setpoint changes established by the higher-level system. The speed controller should provide close tracking the reference signal with no static error, no oscillations and no overshoot. These oscillations and overshoots could cause significant overload or even damage to the mechanical part of the drive. For these reasons we have chosen a simple proportional-integral (PI) controller. A derivative part was omitted because of noise in the input signal. Optimum values of the proportional K_p and integral K_i gains of the controller for the laboratory stand have been selected on the basis of the simulation of the linearized model of the controlled system (inverter-fed induction motor and the mechanical inertia). Model linearization – around the rated operating point – significantly increased the simulation speed, still capturing the most important dynamical features of the original system. Detailed process of controller gain calculation has been presented in [14].

2. Materials and Methods

The squirrel-cage induction motor is, in general, a non-linear element considered over the entire speed range (from start-up to synchronous speed), but in the range of small slips (around the rated slip) corresponding to normal operating conditions under load, it is possible to linearize the mathematical model of this motor by taking into account the slope of the motor's mechanical characteristics and

Publisher: **KOMAG Institute of Mining Technology, Poland**

the electromagnetic and electromechanical time constants. This linearized model enables a relatively fast and efficient simulation of the dynamic waveforms for the purpose of determining the optimum speed controller settings. More detailed but also much more computationally demanding simulation model of motor, converter and gearbox is covered in [15,16]. Such models can be useful for hardware-in-the loop simulation of the control system hardware and software [17]. A simplified block diagram of the whole system is presented in Fig. 2.

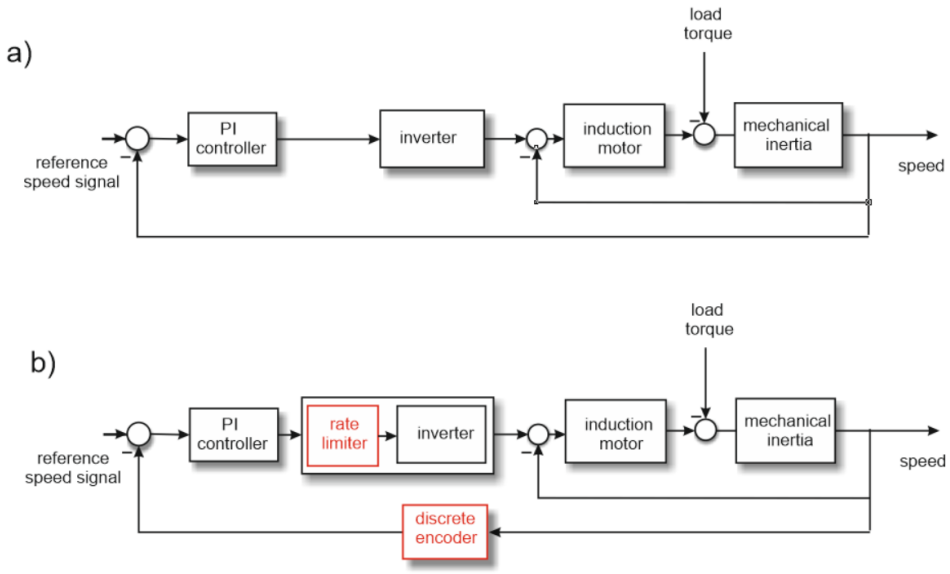

Fig. 2. General block diagram of the roadheader cutting head speed control system: a) simplified linearized model, b) linearized model with added nonlinear elements (marked in red)

Details of the diagram blocks from Fig. 2 (e.g. transfer function formulas, model coefficient values etc.) have been presented in [14].

The frequency converter can also be considered as a linear element with relatively low inertia and a delay of a few or several milliseconds, i.e. negligibly small in comparison with the inertia of the mechanical system (motor rotor, gearbox and cutting head). In this situation, one of the most important elements affecting the dynamics of the entire system is the input filter limiting the rate of the frequency change, mounted at the input of the inverter. The purpose of this filter is to limit the rate of change of the output frequency (and output voltage) of the inverter in order to avoid approaching (or even exceeding) the critical slip value and the associated current overload of the inverter transistors [18,19,20]. The influence of power supply frequency changes on induction motor torque is presented in Fig. 3. Such a rapid torque and current overload can cause the converter to shut down immediately and interrupt the drive system operation.

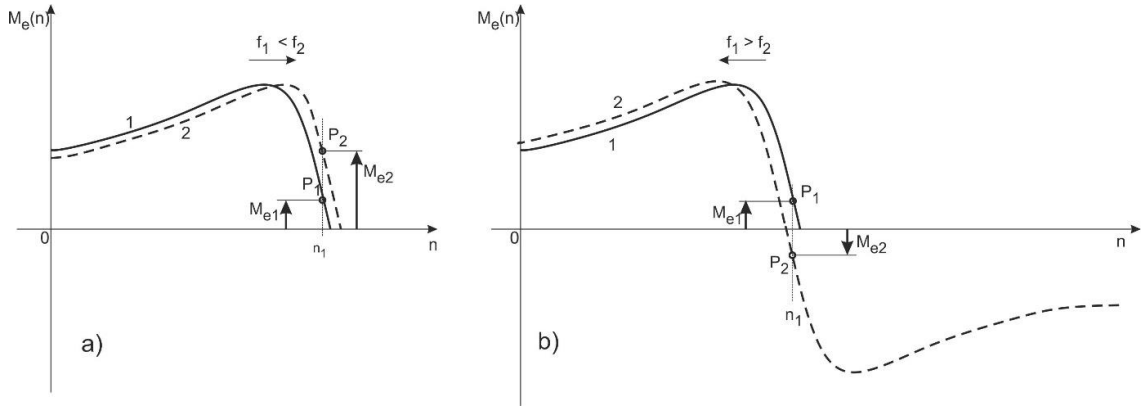

Fig. 3. Influence of power supply frequency changes on induction motor torque (M_{e1}, M_{e2} – torque values corresponding to operating points $P_1(f_1)$, $P_2(f_2)$ for different values of slip): a) at acceleration ($f_1 < f_2$), b) at deceleration ($f_1 > f_2$)

The rate-of-change limiter is a linear element in the static meaning (it carries the full range of frequency variation from zero to the rated frequency), but non-linear in the dynamic meaning (it allows slowly varying signals to pass unchanged, while limiting the variability of high-speed input signals). For an approximate analysis of the operation of a system with such an element, the harmonic linearization method (also known as the descriptive function method) can be used. In contrast to the well-known form of the descriptive function determined for elements with non-linear static characteristics, the form of the function describing dynamically non-linear elements is not reported in the relevant literature [21,22,23]. Its derivation is one of the issues addressed in this test.

The control system fitted to the laboratory stand used a rate limiter set by the inverter manufacturer to a value of $\alpha = 4$ Hz/sec. The signal passing through this limiter is deformed in terms of both amplitude (reduced) and phase (delayed). The principle of these constraints is shown in Fig. 4, and some examples of such variations are shown in Fig. 5.

Fig. 4. Rate-limiter of the input signal

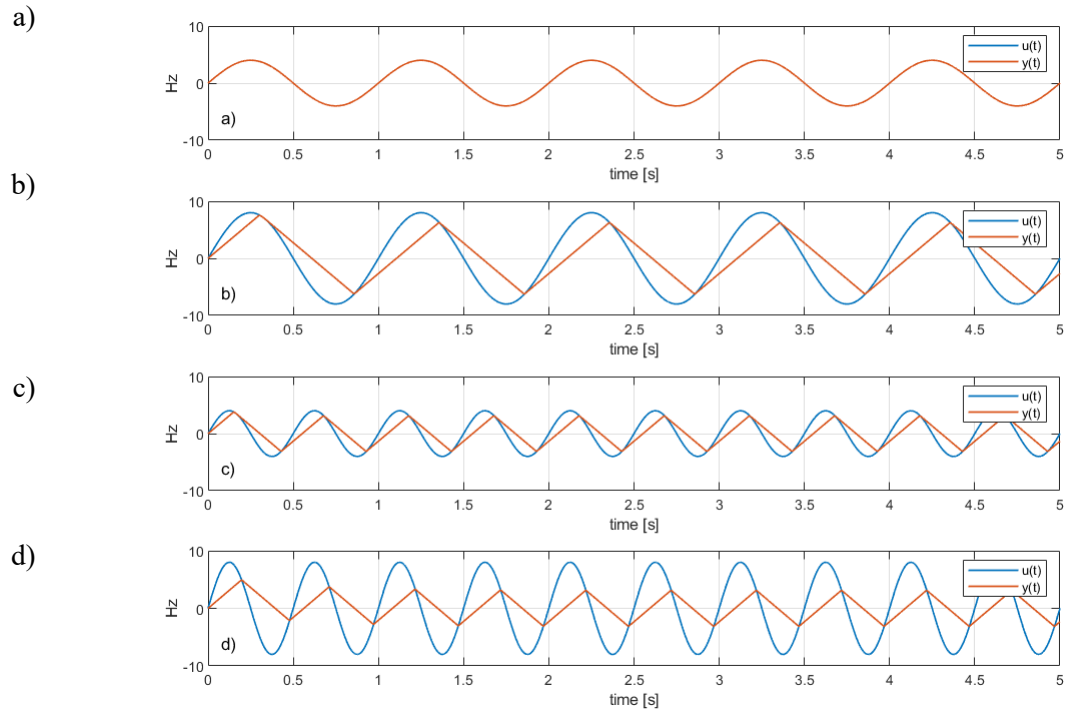

Fig. 5. Examples of the rate-limiter operation:
a) small magnitude, low frequency (no distortion), b) greater magnitude, low frequency,
c) small magnitude, higher frequency, d) higher magnitude, higher frequency

Quantitative analysis of this phenomenon can be carried out on the basis of the situation shown in Fig. 6 and the selected points of intersection of the sinusoidal (input) curve with the triangular (output) curve where α denotes a maximum permissible signal rate. This intersection point marks the peak of the triangular output waveform, so it can be used to compare against the peak of the input sinusoidal

waveform to determine both an amplitude and a phase shift of the triangular output waveform. The condtion of the intersection point can be stated as: $A \cdot \sin[\omega \cdot (t_u + \Delta t_u)]$

$$\underbrace{A \cdot \sin\left[\omega \cdot \left(t_u + \Delta t_u\right)\right]}_{u(t)} = \underbrace{\alpha \cdot \left(t_u + \Delta t_u\right) - \alpha \cdot \Delta t_u}_{y(t)} = \alpha \cdot t_u \tag{1}$$

where:

A – magnitude of the input signal,

ω– angular frequency of the input signal,

Δt_u – time interval between midpoint of the inaput of the waveforma and the intersection point,

t_u - a quarter of the input signal period,

α – maximum permissible rate of the input signal (straight-line directional coeffcient).

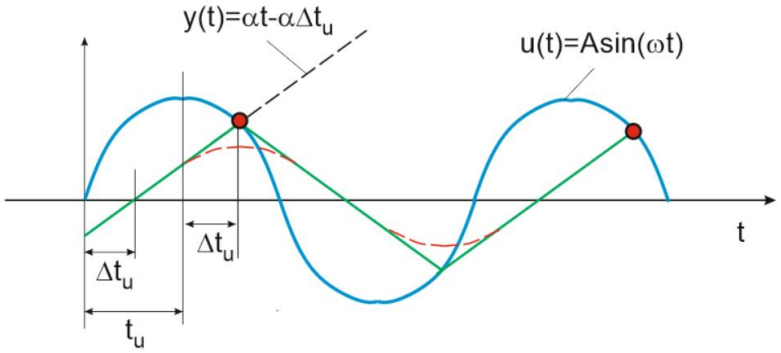

Fig. 6. Graphical analysis of the sinusoidal input waveform (blue) and the triangular output (green) waveforms and their intersection points. The red dashed waveform denotes first harmonic of the output triangular waveform

As the relationship between the time delay Δt_u and corresponding phase-shift φ can be written as:

$$\Delta t_u = \frac{\varphi}{\omega} \tag{2}$$

equation (1) can be stated as:

$$A \cdot \sin\left[\omega \cdot \left(\frac{\pi}{2\omega} + \frac{\varphi}{\omega}\right)\right] = \alpha \cdot \frac{\pi}{2\omega} \tag{3}$$

so:

$$\sin\left(\varphi + \frac{\pi}{2}\right) = \frac{\pi \cdot \alpha}{2\omega \cdot A} \tag{4}$$

and finally, the phase-shift can be expressed as:

$$\varphi(A, \omega) = \arcsin\left(\frac{\pi \cdot \alpha}{2\omega \cdot A}\right) - \frac{\pi}{2} \tag{5}$$

As any triangular function with peak value F and angular frequency ω can be decomposed into a Fourier series of the form [24,25,26]:

$$f(t) = \frac{8F}{\pi^2}\sin(\omega t) - \frac{8F}{(3\pi)^2}\sin(3\omega t) + \frac{8F}{(5\pi)^2}\sin(5\omega t) + ... \tag{6}$$

The peak value of the first harmonic of the triangular output function will therefore depend on both ω and α and will have a value of:

$$Y_m = \frac{8 \cdot (\alpha \cdot t_u)}{\pi^2} = \frac{8\alpha\left(\frac{\pi}{2\omega}\right)}{\pi^2} = \frac{4\alpha}{\omega\pi} \tag{7}$$

Therefore for a complex describing function $\underline{G}(A, j\omega)$ defined as:

$$\underline{G}(A, j\omega) = \frac{\underline{Y}(A, j\omega)}{\underline{U}(A, j\omega)} \tag{8}$$

the gain of the rate limiter calculated as the modulus (absolute value) of the function can be determined as:

$$\left|G(A, j\omega)\right| = \frac{Y_m}{A} = \frac{4\alpha}{\pi \cdot \omega \cdot A} \tag{9}$$

and the phase-shift is defined by eq. (5) as:

$$\varphi = Arg\{\underline{G}(A, j\omega)\} = \arcsin\left(\frac{\pi \cdot \alpha}{2 \cdot \omega \cdot A}\right) - \frac{\pi}{2} \tag{10}$$

Example graphs of $G(A, j\omega)$ function – both modulus (gain) and phase-shift are presented below in Fig. 7 for an example range of input signal peak values and frequencies. They are based respectively on equations (9) and (10). For small and slowly varying input signals the gain equals 1, and the phase shift is 0 – so the signal is not damped. If the input signal has greater magnitude or greater frequency, the gain decreases below 1 and simultaneously the phase delay increases.

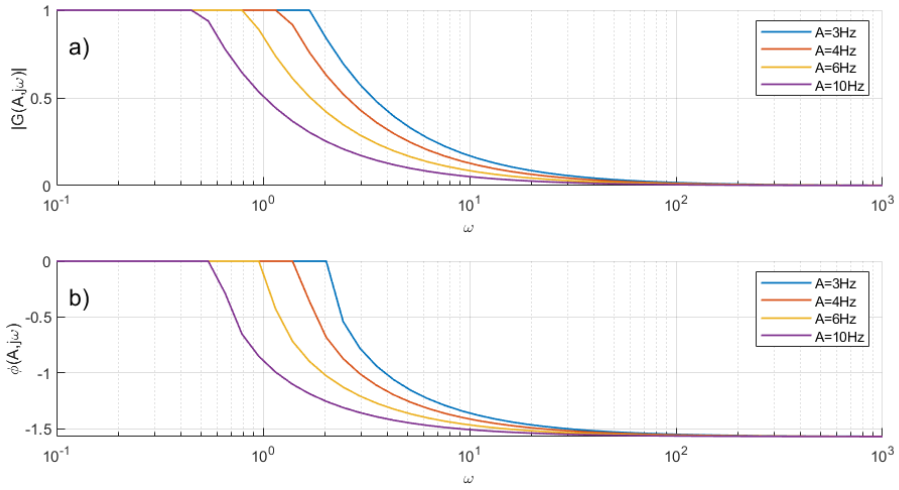

Fig. 7. Frequency input/output curves of the rate limiter (α=4Hz/s) calculated for an example range of input signal peak values: a) gain, b) phase shift

3. Results

The system has been extensively tested at the laboratory stand. There have been presented results of two typical, although qualitatively different tests. The waveform in Fig. 8. is characterized by a large variation of the signal generated by the higher-level reference setter. In this case, the primary task of the speed control system is to track these changes in the reference signal. It can be seen, however, that in many cases its response is too sluggish, which is related specifically to the limitation of the rate of frequency changes and the current overloads that occur during these changes.

Publisher: **KOMAG Institute of Mining Technology, Poland**

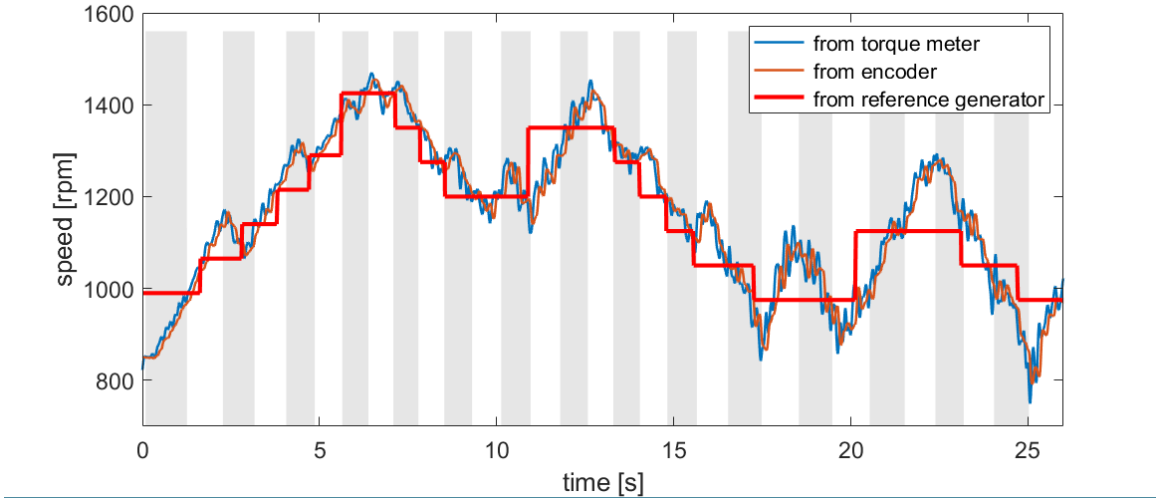

Fig. 8. Example waveform of rotational speed with high reference signal variability recorded at the laboratory stand

In the case of the waveform shown in Fig. 9, there is a distinctive long duration of steady-state operation (occurring after the end of the start-up period). The signal generated by the higher-level reference setter is then featured by a constant level for a longer period of time. Changes in cutting torque caused momentary changes in speed, but the control system maintained the average speed value at the set-point level. Thus, it can be assumed that the disturbances registered in the output signal waveform had the nature of stochastic noise, while the deterministic components have been well suppressed.

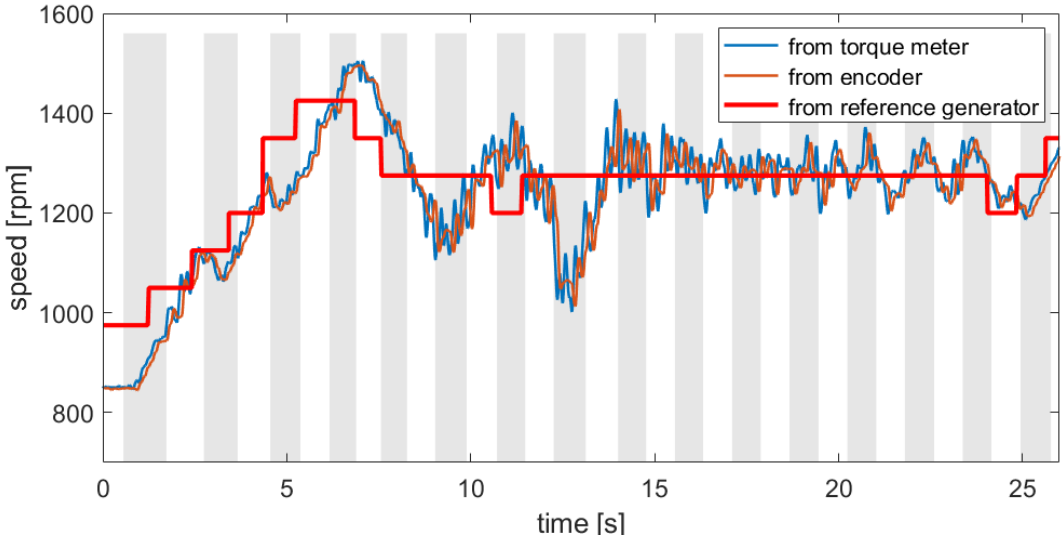

Fig. 9. Example waveform of rotational speed with longer period of constant value reference signal recorded at the laboratory stand

In both Fig. 8 and Fig. 9, there can be seen a small time shift between the speed measurement signals from the torque meter (continuous measurement) and the encoder (discrete measurement). The signal from the encoder is also smoother, which is due to the principle of its operation itself, since the encoder, instead of the instantaneous value, provides the average value of the speed calculated for one full period of rotation of the motor shaft. However, due to the much longer period of operation of the overriding load controller (resulting from the time of one full rotation of the cutting head), which acts as a speed setter, the relatively small delay described above (illustrated in detail by zooming in Fig. 10) does not significantly affect the quality and stability of the control system's operation.

Publisher: **KOMAG Institute of Mining Technology, Poland**

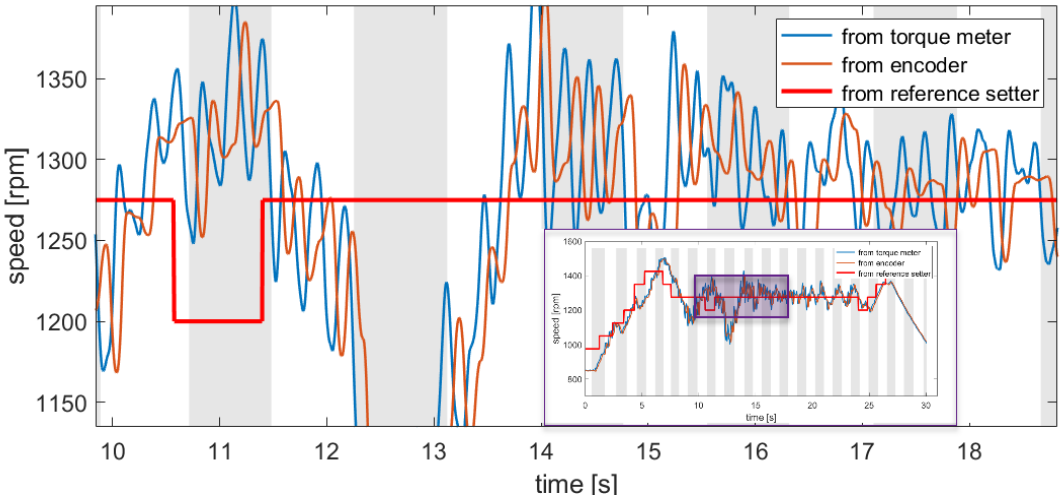

Fig. 10. Part of the recorded waveform from Fig. 8 zoomed in order to distinguish between continuous torque-meter and discrete encoder- based rotational speed signals

4. Conclusions

The PI controller settings determined by numerical optimization methods generally meet their purpose. Disturbances appearing in the system operation system are caused by the adoption of a simplified linearized motor model and the ignoring of additional linear and nonlinear feedback circuits occurring inside the frequency converter. Because of the inverter high thermal sensitivity even to short overloads, the rated power and rated current of the inverter must be greater than resulting from the motor parameters. Also, the internal frequency rate limiter on the input of the frequency converter has a deep impact on overall system dynamics and should be included in modelling, tuning and analysis of the roadheader and its control system model. The parameters of the motor model can also be affected by the change in resistance of the motor windings, caused by their heating during operation. Therefore, it seems purposeful to use other types of controllers - e.g. a robust controller with an internal model of the controlled drive. Slight improvement in following the reference speed signal can be also achieved by better (continuous and non-delayed) speed measurements.

Acknowledgements

The work has been implemented under the research project titled “Control of roadheader cutting heads movement for reduction of energy consumption of mining and dynamic loads“ co-financed by the Polish National Centre for Research and Development under the Applied Research Projects (Agreement No. PBS3/B2/15/2015).

References

[1] Deshmukh S., Raina A.K., Trivedi R.: Roadheader – A comprehensive review. Tunnelling and Underground Space Technology.Vol. 95, January 2020

[2] Jasiulek D., Świder J.: “Mechatronic systems in mining roadheaders – examples of solutions” PAR (Measurements, Automation, Robotics) vol. 17 no. 1, pp 121-127, 2013

[3] Cheluszka P., Remiorz E., Rostami J.: The Use of a Roadheader Simulator in Research of Dynamics and Energy-Consumption of Excavating Underground Roadways and Tunnels. Energies 2022, No15(18), 6673, DOI 10.3390/en15186673

[4] Torano J., Menendez M., Rodriguez R.: Experimental results of a low-power roadheader driving a gallery with .different types of rock at the face. Tunnelling and Underground Space Technology. Vol. 18, August 2003

[5] Tong M.: Kang D., Liu P.: Research on Automatic Section Cutting Control of Roadheader. IEEE

International Conference on Measuring Technology and Mechatronics Automation, 13-14 March 2010

[6] Liu X., Du Ch., Liu M.: Research on spiral angle optimization for longitudinal road header's cutting head. Proc IMechE Part C: J Mechanical Engineering Science 2020, Vol. 234(17) 3346–3359

[7] Chen H., Yang W., Ma Y.: Multi-sensor fusion method for roadheader pose detection, Mechatronics Vol. 80, December 2021

[8] Qi P, Chang J, Chen X, Wang T, Wu M.: Identification of Rock Properties of Rock Wall Cut by Roadheader Based on PSO-VMD-LSSVM. Frontiers in Earth Sci. May 2022, vol. 10

[9] Jasiulek D., Stankiewicz K., Swider J.: An adaptive control system of roadheader with intelligent modelling of mechanical features of mined rock. Journal of KONES Powertrain and Transport, Vol. 18, No. 2 2011

[10] Devy M., Orteu J.J., Mining robotics:: Application of computer vision to the automation of a roadheader. Robotics and Autonomous Systems 1993 Vol. 11

[11] Gao X.:Discussion on the remote visual control technology system of fully-mechanized heading face in mine. IOP Conference Series: Earth and Environmental Science, Vol. 508, Tianjin, 24-26th April 2020

[12] Salsani A., Daneshian J., Shariati S.: Predicting roadheader performance by using artificial neural network. Neural Computing and Applications, Vol. 24, No 7-8, June 2014

[13] Avunduk E., Tumac D., Atalay A.K.: Prediction of roadheader performance by artificial neural network. Tunnelling and Underground Space Technology, vol.44, September 2014

[14] Heyduk A., Joostberens J.: Automatic control of roadheader cutting head speed and load torque. 6th World Multidisciplinary Earth Sciences Symposium (WMESS 2020), 7-11 September 2020, Prague, Czech Republ. IOP Conference Series Earth and Environmental Science, December 2020

[15] Cheluszka P., Kaula R., Heyduk A. and Gawlik J.:Modelling the dynamics of a drive of boom-type roadheader cutting heads at adjustable angular speed. Arch. Mining Sci. vol. 63, pp. 183-204, 2018

[16] Heyduk A., Joostberens J.: Computer simulation of the roadheader cutting head speed control system. 18th International Multidisciplinary Scientific GeoConference: SGEM 2018, 2 July - 8 July 2018, Albena, Bulgaria. Conference proceedings, International Multidisciplinary Scientific GeoConference & EXPO SGEM, 2018, Sofia, STEF92 Technology

[17] Heyduk A., Joostberens J.: Hardware-in-the-Loop simulation applied to roadheader cutting head speed control system testing. Mining - Informatics Automation and Electrical Engineering 4 (532), January 2017.

[18] Jufer M.: Electric Drives: Design Methodology. Wiley-ISTE 2010

[19] Krause P., Wasynczuk P., Sudhoff S,C.: Analysis of Electric Machinery and Drive Systems. IEEE Press Wiley, 3rd Ed. 2013

[20] Razik H.: Handbook of Asynchronous Machines with Variable Speed. Wiley ISTE, London 2011

[21] Gelb A., Vander W E.: Multiple-Input Describing Functions and Nonlinear System Design. McGraw-Hill, 1968

[22] Aguilar L.T.:, Boiko I., Fridman L., Iriarte R: Self-Oscillations in Dynamic Systems: A New Methodology via Two-Relay Controllers. Birkhäuser Basel, 2015

[23] Lurie B., Enright P.: Classical Feedback Control with Nonlinear Multi-Loop Systems: With MATLAB® and Simulink®. Taylor Francis CRC Press, Boca Raton 2020

[24] Dyke P. An Introduction to Laplace Transforms and Fourier Series. Springer London, Heidelberg, 2nd ed. 2017

[25] Hsu T.: Fourier Series, Fourier Transforms, and Function Spaces. A Second Course in Analysis. AMS MAA Press, Providence 2020

[26] Serov V.: Fourier series, Fourier transform and their applications to mathematical physics. Springer London, Heidelberg, 2017

Publisher: **KOMAG Institute of Mining Technology, Poland**